Combustion and Emission Performances of Coconut, Palm and Soybean Methyl Esters under Reacting Spray Flame Conditions

Meng Choung Chiong[a], Cheng Tung Chong[a,b,*], Jo-Han Ng[b,c,d], Manh-Vu Tran[e], Su Shiung Lam[f], Agustin Valera-Medina[g], Mohammad Nazri Mohd Jaafar[a]

[a] Faculty of Mechanical Engineering, Universiti Teknologi Malaysia, 81310 Skudai, Johor, Malaysia.
[b] UTM Centre for Low Carbon Transport in Cooperation with Imperial College London, Universiti Teknologi Malaysia, 81310 Skudai, Johor, Malaysia.
[c] Faculty of Engineering and The Environment, University of Southampton Malaysia, 79200 Iskandar Puteri, Johor, Malaysia.
[d] Energy Technology Research Group, Engineering Sciences, University of Southampton, SO17 1BJ, Hampshire, UK.
[e] School of Engineering, Monash University Malaysia, Jalan Lagoon Selatan, 47500 Bandar Sunway, Selangor, Malaysia.
[f] Eastern Corridor Renewable Energy Group (ECRE), Environmental Technology Programme, School of Ocean Engineering, Universiti Malaysia Terengganu, 21030 Kuala Terengganu, Terengganu, Malaysia.
[g] College of Physical Sciences and Engineering, Cardiff University, Wales, United Kingdom.

Abstract

The spray combustion characteristics of coconut (CME), palm (PME) and soybean (SME) biodiesels/methyl esters were compared with diesel by using an axial swirl flame burner. Atomisation of the liquid fuels was achieved via an airblast-type nozzle with varied atomising air-to-liquid ratios (ALR) of 2-2.5. The fully developed sprays were mixed with strongly swirled air to form combustible mixtures prior to igniting at the burner outlet. Under fuel-lean condition, biodiesel spray flames exhibited bluish flame core without the yellowish sooty flame brush, indicating low sooting tendency as compared to baseline diesel. Increasing the atomising air led to the reduction of flame length but increase in flame intensity. Measurements of post-combustion emissions show that SME produced higher NO as compared to CME and PME due to higher degree of unsaturation, while the most saturated CME showed the lowest NO and CO emissions amongst the biodiesels tested across all equivalence ratios. By preheating the main swirl air to 250 ^{o}C, higher emissions of NO, CO and CO_2 were observed for biodiesels. Higher ALR led to reduced NO and CO emissions regardless of the fuel used, making it a viable strategy to resolve the simultaneous NO-CO reduction conundrum. This work shows that despite different emission characteristics exhibited by biodiesels produced from different feedstock, they are in principle potential supplemental fuels for practical combustion systems. The higher pollutant emitted can be mitigated by operating at higher ALR in a twin-fluid based swirl combustor.

Keywords: Biodiesel; Soy; Palm; Coconut; Spray flame; Emissions

*Corresponding author
Address: Faculty of Mechanical Engineering, Universiti Teknologi Malaysia 81310 Skudai Johor, Malaysia.
Email: ctchong@mail.fkm.utm.my ; Phone: +60(7) 5534631 ; Fax: +60 (7) 5566159

1. Introduction

The recent energy outlook report by the International Energy Agency (IEA) has projected the energy dependent on biodiesels to grow from 0.83 EJ in 2015 to 5.97 EJ by the year 2035 [1]. The growing importance of biodiesel stems from the global decarbonising efforts, as the renewable fuel forms a closed-carbon cycle as opposed to the open-carbon cycle when utilising petroleum diesel [2]. Additionally, the use of biodiesel in combustion applications is comparatively cleaner than that of fossil diesel in terms of lower particulate matter (PM), sulphur dioxide (SO_2) and unburnt hydrocarbon (UHC) emissions [3,4]. While there are other alternative fuels that are also cleaner than fossil diesel in combustion application, biodiesel stands in the forefront as it can use existing diesel infrastructures and distribution channels [5]. This is due to its similar caloric value, viscosity and cetane number with diesel [6,7]. This has led to the widespread interest of applying biodiesel in reciprocating combustion engine for the transportation sector [8–10].

Fuel-flexible gas turbine is envisaged from the standpoint of reducing operating cost, while also meeting emissions targets. Biodiesel has been identified as one of the prospective alternative fuels for gas turbines. Biodiesel-fuelled gas turbines have been experimentally studied using lab-based swirl flame burners or actual gas turbine engines. A study on the spray and combustion properties of rapeseed biodiesel using a gas turbine-type burner concluded that, biodiesel spray exhibited longer spray penetration length and smaller spray cone angle as compared to that of diesel [11]. The phenomena are attributed to the higher density, viscosity, surface tension and boiling point of biodiesel as compared to that of conventional diesel fuel. It has also been found that biodiesel produced lower NO_x (nitrogen oxides) emissions by 21% when compared to that of diesel at an axial distance of 60 mm from the nozzle. This suggested that spray atomisation plays an important role in NO_x emissions. In another study using gas turbine swirl flame burner, it was again demonstrated that higher atomisation pressure resulted

in finer spray with smaller droplet size and subsequently lower NO_x emissions [12]. The NO_x emissions level was decreased from 13 ppm to 9 ppm as atomising pressure was increased from 0.4 to 0.8 MPa. The increase in droplet size causes larger number of droplets to be transported downstream of the flame, thus requiring longer evaporation time. Consequently, the ratio of combustion in diffusion mode to premixed mode increases, leading to greater incidences of the local regions with high temperatures, in turn causing greater amount of NO_x formed [12,13].

In a study that examined rapeseed biodiesel with swirl flame burner, it was demonstrated that rapeseed biodiesel's nitric oxide (NO) emissions were reduced by approximately 22% as compared to that of diesel, at 6 kW output power. It was postulated that the higher heat of vaporisation of the biodiesel spray and the presence of oxygen in the fuel may partially suppress the prompt NO formation mechanism [14]. In other related studies, carbon monoxide (CO) emission for biodiesel derived from soybean was reported to reduce by 50% as compared to that of diesel under fuel-mass specific by using a swirl burner equipped with an airblast type atomiser [15]. By utilising a flow blurring injector, it was demonstrated that mixing was improved and CO emissions of biodiesel flame could be reduced by 2-3 times when ALR was varied from 2.0 to 2.4 [16].

Applications of biodiesel in micro gas turbine (MGT) have been conducted by several other groups. In a study using a Capstone C30 MGT, soybean biodiesel was reported to cut down NO_x emissions by 60% as compared to that of fossil diesel [17]. However, in another study that utilised the same MGT model, soybean biodiesel was found to produce higher NO_x against that of diesel [18]. The higher NO_x emission from biodiesel was attributed to the larger biodiesel droplet size that led to the longer evaporation time scale that promotes NO_x emission [18]. In addition, the performances of soybean, canola, recycled rapeseed biodiesel and hog-fat biofuel against Jet A fuel were also investigated using a 30 kW gas turbine engine [19]. It was found that NO emissions for biodiesel were consistently lower than that of diesel for

equivalence ratio range of 0.15 to 0.30, with a maximum reduction of up to 75%, in spite of the similar turbine inlet and exhaust gas temperature for both biodiesel and diesel. Hence, it was postulated that NO_x formation in that instant was not dominated by thermal NO mechanism. CO emissions were found to be lower for biodiesels as the fuel-bound oxygen in the biodiesel assists in converting CO into CO_2 [19,20].

The thermal performance and emissions of a 30 kW MGT when fuelled with highly viscous castor biodiesel were compared with baseline diesel [21]. It was demonstrated that CO emission increased by 50% as compared to diesel at 14 kW engine output power, due to the inferior atomisation as a result of the high viscosity of castor biodiesel [21]. The authors also opined that the lower NO_x emissions achieved in the MGT tests are partly contributed by the same factor which results in lower combustion temperature. The size of castor biodiesel liquid droplets and primary-zone equivalence ratio are larger when compared with that of diesel. The reduction of temperature in the primary combustion zone (due to higher equivalence ratio) reduced the emission levels of the NO_x pollutants for biodiesel [21]. The emissions of 15% and 25% jatropha biodiesel-diesel blends were compared with neat diesel using a Rover gas turbine IS/60 test rig, where the blends showed higher emissions of NO_x by 34-42% as compared to that of diesel at the same power output [20]. It was postulated that the higher oxygen content in biodiesel led to higher flame temperature and subsequently higher level of NO_x emissions [20].

Applications of biodiesel in actual gas turbines have been conducted by several groups. The ignition, combustion dynamics and emissions of biodiesel in an industry gas turbine (Siemens SGT-100) were conducted by Liu et al. [22]. The NO_x emissions for biodiesel were found to be lower than that of diesel for all operating conditions tested. In another study, Moliere et al. [23] reported no smoke and sulphur oxide were emitted when the industrial gas

turbine (GE 6531B) was fuelled with biodiesel. These field tests indicate the positive effects of biodiesel towards the environment.

The variations in biodiesel feedstock, combustion chamber geometries, interaction between fuel spray and swirling air from the aforementioned studies have led to conflicting reports on the combustion and emissions characteristics of biodiesel usage in gas turbines. Additionally, most of the studies were conducted for the single feedstock biodiesel in isolation and without direct comparison against biodiesel from other feedstock within the same experimental studies.

Thus, this study adopts a multi-feedstock approach for an experimental investigation of biodiesel produced from coconut (CME), palm (PME) and soybean (SME) using a lab-based gas turbine type swirl burner operated at atmospheric condition. The study mainly investigates the effects of preheated air temperature, atomiser air-to-liquid (ALR) ratio, global equivalence ratio (ϕ) and degree of unsaturation level in biodiesels on the combustion and emissions characteristics of a model gas turbine swirl flame burner fitted with a twin-fluid nozzle. Fossil diesel is used as baseline fuel in this study.

2. Experimental setup

2.1 Operating fuels

The fuels used in this experimental study were coconut (CME), palm (PME) and soybean (SME) biodiesels, with fossil-based diesel as the baseline. Diesel was procured from a local gas station, while the tested biodiesels were produced from their respective vegetable oil counterparts in the lab via the transesterification process. The vegetable oils were reacted with methanol catalysed by potassium hydroxide (KOH) for 2 hours using a magnetic stirrer, with temperature maintained at 60 °C. The mass ratio of the vegetable oil:methanol:KOH was fixed at 113.75:50:1. Decanting was carried out to allow for the separation of reaction products

to remove glycerol and catalyst from the biodiesel. The produced biodiesel was then heated up to 120 °C for 4 hours to allow the evaporation of residual water and methanol.

A gas chromatograph (Agilent 7820A) was used to characterise the biodiesel. The composition for the CME, PME and SME produced are shown in Table 1. It can be observed that SME contains a substantial amount of unsaturated fatty acid with double bond at 83.87 wt%, while CME is mostly composed of saturated fatty acid with single bond at 92.82 wt%.

Physical properties for the tested fuels are shown in Table 2. Biodiesel is more viscous and less volatile as compared to diesel. The higher flash point of biodiesel results in lower volatility than diesel. Biodiesels also have lower calorific value of around 12.2-17.3% by mass, and 9.1-14.3% by volume as opposed to that of fossil diesel. This is due to the presence of fuel-bound oxygen content of in the range of 9.7-14.4% by weight for biodiesel.

2.2 Swirl Burner System

Fig. 1 illustrates the schematic diagram for the experimental setup. A gas turbine type swirl burner was used to establish a steady liquid spray flame. The axial swirler placed concentrically at the burner outlet consists of 6 straight vanes with the angle of 45°, forming the geometric swirl number of 0.84 based on Eq. 1 [24].

$$S_N = \frac{2}{3}\left[\frac{1-\left(D_h/D_s\right)^3}{1-\left(D_h/D_s\right)^2}\right]\tan\theta \qquad (1)$$

where D_h and D_s are the diameters of the swirler hub and the swirler, respectively. The angle of the swirl blade from the centreline is denoted by θ. A swirling air flow that envelopes the atomised spray is formed when the main air passes through the swirler, forming a combustible

mixture. The swirler generates a high intensity recirculating flow to assist in fuel-air mixing and flame stabilisation.

The liquid fuel was delivered by a peristaltic pump (Longer BQ50-1J) and a flow damper was utilised to damp out the pulsating flow ripple caused by the peristaltic motion. Silicone tube with an inner diameter of 4 mm was used for the peristaltic pump to transfer the fuel. Prior to mixing with main swirling air, the fuel was atomised by a commercial twin-fluid atomiser (Delavan: SN type-30610-1). The atomising air and fuel orifice diameters are 1.73 and 0.50 mm, respectively. The supply of the atomising air and combustion air were controlled by air mass flow controllers (Sierra SmartTrak 50).

For the preheating of the main air, three rope heaters (Omega: FGR-100–240V) with a rated output of 500 W were used. The burner's plenum was insulated with heat resistant ceramic wool to minimise heat loss. A 1.5 mm K-type thermocouple was placed 10 mm upstream of the burner to measure the temperature of the preheated main air flow. This thermocouple provides feedback to the Proportional-Integral-Derivative (PID) controller to regulate the heating process. Flue gas from the combustion was directed to the exhaust by a 400 mm long, 130 mm diameter flame tube made from carbon steel, as depicted in Fig. 1.

2.3 Measurement techniques

2.3.1 Flame Imaging

A Canon EOS 600D digital camera was utilised to acquire the global flame images through a quartz wall that is optically accessible. Focal length and exposure time of 4 mm and 1/15 s, respectively, were used to capture the flame images.

2.3.2 Gas analyser

A gas analyser (KANE; KM9106 Quintox) was used to measure the concentrations of post-combustion NO, CO and CO_2 products in the flue gas at the outlet of combustor. The sampling was carried out by placing the probe 13 mm inward from the combustor exit. Emissions were measured at 5 spatial locations that were radially and equally spaced. Calibration gases were used to check the accuracy of the gas analyser before measurements. The sampling probe is 5 mm in diameter and the gas analyser sampled the flue gas at the rate of 2 L/min. The NO and CO emissions were measured via chemical sensors in the gas analyser, while the CO_2 emissions were calculated based on the measured oxygen (O_2). The probe sampled for 90 seconds at each spatial location to ensure steady state readings. The final global emissions for each test case were obtained by averaging the spatial readings using the area-weighted averaging method. The measurement range, resolution and propagated error for NO, CO, CO_2 and O_2 are summarised in Table 3.

2.4 Operating conditions

The liquid fuels and atomising air were independently delivered to the burner outlet at room temperature. The main combustion air was preheated to 250 °C prior to its mixing with the liquid fuel spray. Fuel flow rate was adjusted for each fuel to achieve a fixed power output of 9.3 kW. The atomisation air-to-liquid ratio (ALR) was varied at 2.00, 2.25 and 2.50 by regulating the flow rate of atomising air while holding the fuel flow rate constant. The ALR of 2.00 was chosen as the lower limit as it is near the limit of ALR where atomising air is adequate to produce proper spray [26]. For each of the ALR, the equivalence ratio was varied from 0.65 to 0.90 to simulate lean combustion regime in gas turbine. The mass flow rates for combustion air and fuel at equivalence ratio 0.65 are shown in Table 4 for different fuels.

3. Results and Discussion

3.1 Reacting Spray Imaging

The flame appearances for diesel, PME, SME and CME established at ALR=2.50 for equivalence ratios of $\phi = 0.90$ and 0.65 are shown in Fig. 2. It is shown that downstream region of the diesel main reaction zone is occupied by a distinct orange-yellow luminous flame, while biodiesels show mainly bluish flames. The orange-yellow luminous flame is due to the burning of soot particles in this region. Soot consists of aromatic structure, therefore fuels that contain substantial amount of aromatics structure in its chemical composition, such as diesel, is expected to be sootier than those from biodiesels [27]. Soot production was shown to increase linearly with increasing aromatic contents in the fuel [27]. On the other end, bluish flame at the verge of nozzle outlet is equivalent to the premixed flame caused by internal mixing between the atomising air and fuel. The presence of bulk oxygen increases oxidation rate of soot particles, resulting in reduced luminous orange-yellow sooty flame [28].

In contrast to diesel, biodiesels show distinctively different spray flame appearance with the notable absence of sooty orange at their post-reaction zones for the higher ALR cases. The absence of aromatics structure in biodiesels also greatly reduces the soot formation tendencies in biodiesels, due to the lack of the soot precursors. The fuel-bound oxygen content for the fatty acid methyl ester molecules also promotes soot oxidation, which is another reason for lower soot production in biodiesel spray flames [28]. By reducing the ALR to 2.0, inferior atomisation results in poorer mixing between reactants and air. This consequently incurs substantial soot formation due to incomplete combustion. The increase of soot formation at lower ALR is shown in Fig. 3 by the distinctively larger orange-yellow flame brush for all fuels.

Apart from the fuel properties, the dynamics of the flow also affects the flame appearance. A notable structure in a typical swirl stabilised flame is the presence of central toroidal recirculation zone (CTRZ) [29]. CTRZ plays essential role in stabilising the flame as

it recirculates the hot flue gas back into the reaction zone to constantly heat up the reactants. The presence of CTRZ directs the fuel spray towards the radial direction, forming a dual shear layer. The shear layer is the region where mixing and reaction of the reactant and oxidiser take place [29]. The presence of dual shear layer is notable for biodiesels spray flame. For diesel, however, the appearance of shear layer is overshadowed by the sooty orange-yellow flame. At lower equivalence ratio, greater amount of air flow generates a more concentrated CTRZ that subsequently moved the stagnation point towards upstream position to form a heart-shape reaction flame core.

3.2 Post-combustion Emissions

3.2.1 Effect of Main Swirl Air Temperature

The emissions of NO as a function of equivalence ratio at elevated main air temperature of 30 and 250 °C are shown in Fig. 4. Higher level of NO emission was shown for all fuels tested at elevated main air temperature. The energy provided from the preheated air assists the species molecules to surpass the energy threshold easier for chemical reactions, thus enabling greater amount of energy release with higher flame temperature that subsequently leads to higher NO [30]. Fuel wise, biodiesels exhibit generally higher NO emission as compared to that of diesel for both 250 ^{o}C and 30 ^{o}C main air temperatures. The main exception would be the highly saturated CME. This is postulated to be due to biodiesels possessing larger droplets size and lower volatility as compared to diesel, leading to longer droplets residence time [24]. Longer droplets residence time subsequently promotes thermal NO formation. Apart from thermal NO, prompt NO constitutes another portion of NO emission. The formation of prompt NO depends very much on methylidyne (CH) radical, which serves as the precursor for prompt NO formation [30]. It was shown that biodiesels produced more CH radical than diesel, which

inherently elevates prompt NO formation as compared to diesel [30,31]. The elevation of both thermal and prompt NO result in higher NO emission for biodiesel as compared to diesel.

It can be observed that SME produced the highest NO, followed by PME and CME for the preheated main air temperature cases at ALR = 2.5 and power output of 9.3 kW. The trend of NO emission was found to correlate with unsaturation degree of the biodiesels, where highly unsaturated biodiesel (SME) produces more NO emissions as compared to that of the saturated biodiesel (CME). This is in due to the double bond in unsaturated biodiesel that releases more energy when breaking up as compared to single bond, thus inherently increased adiabatic flame temperature and thermal NO formation [32]. In addition, highly unsaturated biodiesels also promote the formation of CH radicals that serve as the precursor for prompt NO formation, which is another reason that contributes to higher NO emissions [31]. Such trends were not observed for the non-heated main air flow cases where PME produced greater NO emissions than that of the more unsaturated SME.

The CO emissions from biodiesels were generally higher than that of diesel throughout the equivalence ratios investigated for both non-heated and preheated main air conditions, as shown in Fig. 5. Larger fuel droplets and lower fuel volatility of biodiesel inhibit complete combustion, which consequently results in greater CO emission as compared to that of diesel. SME and PME that possess higher viscosity and lower volatility result in higher CO emission as compared to CME. This is due to the higher viscosity and lower fuel volatility slowing down droplet vaporisation rate, subsequently hindering the complete combustion process. At higher preheating temperature, the CO emission level is lower than non-heated case by approximately a factor of 2, which is a reverse trend of NO (Fig. 4). This is expected as preheated air promotes higher efficiency in combustion with higher flame temperature that increases NO but lowering the CO.

The effect of equivalence ratio on the NO and CO emissions are elucidated in Fig. 4 and Fig. 5, respectively. At $\phi = 0.9$, the relatively lower main air flow reduces the turbulence intensity that consequently weakens the CTRZ. This causes poorer mixing and increases the CO emission. As more air is introduced, the overall mixture equivalence ratio is reduced, hence strengthening the CTRZ due to increased swirl intensity that promotes the mixing between the reactants and oxidiser. A more complete combustion is achieved whereas CO emission is reduced substantially. Minimum CO typically occurs at equivalence ratios between 0.7 and 0.8.

Increasing the main air further generates an even stronger CTRZ that recirculates post combustion products back to the flame root. As a consequent, a lower temperature region is formed around the central region of the flame that is in contact with the recirculated gases [29]. The rate of chemical reaction is suppressed in this region due to the lower temperature. CTRZ now weakens the chemical reaction rate instead of promoting the combustion, as indicated by slight CO increment below $\phi = 0.7$. As shown in Fig. 4, maximum NO is produced within the equivalence ratio range, where minimum CO is produced for all fuels. It is hence observable that NO-CO has a distinct trade-off relationship.

The effect of main air temperature on CO_2 emissions is shown in Fig. 6 for diesel and biodiesels. Overall, elevating the main air temperature leads to increase of CO_2 emissions, as a result of increased flame temperature and enhanced CO oxidation rate into CO_2. [30]. As the fuel/air mixture approaches stoichiometric condition, CO_2 concentration increases due to conversion of more carbon from the fuel into CO_2. Higher CO_2 was shown by biodiesels as compared to diesel, partly in due to the increased mass flow rate of fuel to compensate for the lower energy density, as more carbon on a mass basis from the heavier biodiesel chain contributes to the formation of CO_2 during reaction. Among the biodiesels, the unsaturated SME shows higher CO_2 emissions as compared to PME and CME, similar to the trend of NO emissions.

3.2.2 Effect of Air-Liquid Ratio (ALR)

Variation of the ALR imposes significant effects on the emissions. The NO emission is reduced by up to a factor of 2 for the three biodiesels when the ALR is increased from 2.0 to 2.5, as shown in Fig. 7a. The reduction of NO emissions for diesel is less pronounced than those from biodiesel fuels. At lower ALR, inadequate supply of atomising air results in inferior atomisation due to relatively low momentum of air in breaking up the spray. Formation of dense fuel-rich mixture in the spray core inhibits effective heat transfer to the droplets [33]. Fuel droplets that are not fully vaporised are dispersed away by the surrounding air flow. As a consequent, flammable mixture is formed at some distance away from the spray periphery, causing it to burn in diffusional mode which leads to the increase of local flame temperature that promotes thermal NO formation [30]. Conversely, at higher ALR, strong atomising air momentum imparted on the liquid jet produces fine droplets. The sparsely distributed droplets allow greater amount of oxygen to penetrate into the drops cloud [34], where the turbulent flow subsequently accelerates droplet vaporisation rate [33].

A uniform reduction trend of CO emission for all fuels tested was seen with increasing ALR as shown in Fig. 7b. At lower ALR, inferior atomisation forms dense fuel-rich spray with minimum oxygen penetration, causing locally fuel-rich combustion due to the lack of oxygen for complete combustion, thus leading to the increase of CO formation. Fig. 7c shows that CO_2 concentration tends to be slightly higher at ALR=2.0 as compared to ALR=2.5. This could be due to higher combustion temperature at ALR=2.0 that accelerates the oxidation rate from CO into CO_2 [30]. The higher O_2 at ALR=2.5 (Fig. 7d) contributes to the lower NO as lower flame temperature is attained at the spray centreline region. Better mixing was achieved at ALR=2.5 that contributes to the reduction of CO as more efficient combustion is enabled.

Interestingly, biodiesels exhibit higher NO, CO and CO_2 than baseline diesels at all ALR tested, which corroborates with the results shown in previous section. SME shows higher NO, CO and CO_2 among all biodiesels, indicating the effect of unsaturation in the molecule is evident during reaction. CME shows the lowest NO and CO emissions among biodiesels but still displaying higher amount than that of baseline diesel. Despite the higher emissions characteristics for biodiesels, increasing the ALR is an effective way of reducing NO and CO to the level comparable to diesel.

4. Conclusion

In this experimental study, the emission characteristics of PME, SME and CME were compared against that of fossil diesel under the same output flame power of 9.3 kW. The main findings from the study are:

a. diesel flame shows a distinct luminous orange-yellow flame at the downstream of the main reaction zone, whereas all of the biodiesels tested show mainly bluish flames. The luminous orange-yellow flame indicates the presence of soot in the diesel spray flame, which is almost absent in biodiesel spray flames.
b. by increasing the main air temperature, chemical reaction rate accelerates and subsequently increases the production of NO. Conversely, CO emission is reduced due to incomplete combustion.
c. comparison of the NO emission profiles shows that biodiesels produce higher NO compared to diesel. The NO formation in biodiesel is due to higher adiabatic flame temperatures and prolonged droplet residence time that give rise to the thermal NO formation.

d. NO and CO emissions comparison among the three biodiesels shows that highly unsaturated biodiesel (SME) exhibits higher NO production tendency than saturated biodiesel (CME).

e. from a physical property perspective, biodiesel with higher viscosity and lower fuel volatility such as SME produces greater amount of CO as compared to that of CME.

f. a clear trade-off characteristic between NO-CO can clearly be observed when varied against equivalence ratio at a fixed ALR and air temperature.

g. by varying the ALR, the emission profiles are altered, whereby an increase of ALR leads to the simultaneous reduction of NO, CO and CO_2. The study shows that atomisation method and fuel properties directly influence the combustion behaviour, which consequently affects the formation rate of final emissions products.

h. biodiesels have been shown to be suitable supplemental fuels in combustion systems that employ swirl flames such as gas turbines, furnaces and boilers. The higher emissions of biodiesels can be effectively mitigated by utilising the strategy of higher ALR in a twin-fluid atomiser based combustor.

Acknowledgement

Financial support from the Malaysian Ministry of Higher Education and Universiti Teknologi Malaysia (Research University Flagship Grant vote no. 03G63) is gratefully acknowledged.

References

[1] IEA, Technology Roadmap: Delivering Sustainable Bioenergy, 2017.

[2] J.H. Ng, H.K. Ng, S. Gan, Recent trends in policies, socioeconomy and future directions of the biodiesel industry, Clean Technol. Environ. Policy. 12 (2010) 213–238.

[3] V. Soloiu, M. Dunggan, S. Harp, B. Vlcek, D. Williams, PFI (port fuel injection) of n-butanol and direct injection of biodiesel to attain LTC (low temperature combustion) for low-emissions idlingin a compression engine, Energy. 52 (2013) 143–154.

[4] V. Soloiu, J.D. Moncada, R. Gaubert, M. Muiños, S. Harp, M. Ilie, A. Zdanowicz, G. Molina, LTC (low-temperature combustion) analysis of PCCI (premixed charge compression ignition) with n-butanol and cotton seed biodiesel versus combustion and emissions characteristics of their binary mixtures, Renew. Energy. 123 (2018) 323–333.

[5] M. Çetinkaya, Y. Ulusoy, Y. Tekìn, F. Karaosmano□lu, Engine and winter road test performances of used cooking oil originated biodiesel, Energy Convers. Manag. 46 (2005) 1279–1291.

[6] R. Alloune, M. Balistrou, S. Awad, K. Loubar, M. Tazerout, Performance, combustion and exhaust emissions characteristics investigation using Citrullus colocynthis L. biodiesel in DI diesel engine, J. Energy Inst. 91 (2016) 434–444.

[7] J. Thangaraja, K. Anand, P.S. Mehta, Biodiesel NOx penalty and control measures - A review, Renew. Sustain. Energy Rev. 61 (2016) 1–24.

[8] C.T. Chong, J.-H. Ng, S. Ahmad, S. Rajoo, Oxygenated palm biodiesel: Ignition, combustion and emissions quantification in a light-duty diesel engine, Energy Convers. Manag. 101 (2015) 317–325.

[9] H. Chen, Q. Guo, X. yi Zhao, M. long Xu, Y. Ma, Influence of fuel temperature on combustion and emission of biodiesel, J. Energy Inst. 89 (2016) 231–239.

[10] H. Chen, J. He, Y. Chen, H. Hua, Performance of a common rail diesel engine using biodiesel of waste cooking oil and gasoline blend, J. Energy Inst. (2017) 1–11.

[11] L. Li, X. Zhang, Z. Wu, J. Deng, C. Huang, Experimental study of biodiesel spray and combustion characteristics, Powertrain Fluid Syst. Conf. Exhib. (2006).

[12] N. Hashimoto, Y. Ozawa, N. Mori, I. Yuri, T. Hisamatsu, Fundamental combustion characteristics of palm methyl ester (PME) as alternative fuel for gas turbines, Fuel. 87 (2008) 3373–3378.

[13] H. V. Panchasara, B.M. Simmons, A.K. Agrawal, S.K. Spear, D.T. Daly, Combustion Performance of Biodiesel and Diesel-Vegetable Oil Blends in a Simulated Gas Turbine Burner, J. Eng. Gas Turbines Power. 131 (2009) 31503.

[14] C.T. Chong, S. Hochgreb, Flame structure, spectroscopy and emissions quantification of rapeseed biodiesel under model gas turbine conditions, Appl. Energy. 185 (2017) 1383–1392.

[15] D. Sequera, A.K. Agrawal, S.K. Spear, D.T. Daly, Combustion Performance of Liquid Biofuels in a Swirl-Stabilized Burner, J. Eng. Gas Turbines Power. 130 (2008) 32810.

[16] B.M. Simmons, A.K. Agrawal, Combustion Science and Technology Flow Blurring Atomization for Low- Emission Combustion of Liquid Biofuels, Combust. Sci. Technol. 184 (2012) 660–675.

[17] C.R. Krishna, Performance of the Capstone C30 Microturbine on Biodiesel Blends, (2007) 1–11.

[18] C.D. Bolszo, V.G. McDonell, Emissions optimization of a biodiesel fired gas turbine, Proc. Combust. Inst. 32 (2009) 2949–2956.

[19] Z. Habib, R. Parthasarathy, S. Gollahalli, Performance and emission characteristics of biofuel in a small-scale gas turbine engine, Appl. Energy. 87 (2010) 1701–1709.

[20] A. Rehman, D.R. Phalke, R. Pandey, Alternative fuel for gas turbine: Esterified jatropha oil-diesel blend, Renew. Energy. 36 (2011) 2635–2640.

[21] M.A.R. Nascimento, E.S. Lora, P.S.P. Corrêa, R. V. Andrade, M.A. Rendon, O.J. Venturini, G.A.S. Ramirez, Biodiesel fuel in diesel micro-turbine engines: Modelling and experimental evaluation, Energy. 33 (2008) 233–240.

[22] K. Liu, J.P. Wood, E.R. Buchanan, P. Martin, V.E. Sanderson, Biodiesel as an Alternative Fuel in Siemens Dry Low Emissions Combustors: Atmospheric and High Pressure Rig Testing, J. Eng. Gas Turbines Power. 132 (2010) 11501.

[23] M. Moliere, E. Panarotto, M. Aboujaib, J.M. Bisseaud, A. Campbell, J. Citeno, P.-A. Maire, L. Ducrest, Gas turbines in alternative fuel applications: Biodiesel field test, Proc. Asme Turbo Expo 2007, Vol 1. (2007) 397–406.

[24] C.T. Chong, S. Hochgreb, Spray combustion characteristics of palm biodiesel, Combust. Sci. Technol. 184 (2012) 1093–1107.

[25] S.K. Hoekman, A. Broch, C. Robbins, E. Ceniceros, M. Natarajan, Review of biodiesel composition, properties, and specifications, Renew. Sustain. Energy Rev. 16 (2012) 143–169.

[26] C.T. Chong, S. Hochgreb, Effect of Atomizing Air Flow on Spray Atomization of an Internal-Mix Twin-Fluid Atomizer, At. Sprays. 25 (2015) 657–673.

[27] F. Cignoli, S. De Iuliis, G. Zizak, Soot load versus aromatic concentration in diesel oil premixed flames, Fuel. 80 (2001) 945–955.

[28] W. Merchan-Merchan, S. McCollam, J.F.C. Pugliese, Soot formation in diffusion oxygen-enhanced biodiesel flames, Fuel. 156 (2015) 129–141.

[29] J. Kwark, Y. Jeong, C. Jeon, Effect of Swirl Intensity on the Flow and Combustion of a Turbulent Non-Premixed Flat Flame, Flow, Turbul. Combust. 73 (2004) 231–257.

[30] A.H. Lefebvre, D.R. Ballal, Gas Turbine Combustion: Alternative Fuels and Emissions, 3rd ed., CRC Press, 2010.

[31] B. Bazooyar, S.H. Hashemabadi, A. Shariati, NOx formation of biodiesel in utility power plant boilers; Part B. Comparison of NO between biodiesel and petrodiesel, Fuel. 182 (2016) 323–332.

[32] E. Cecrle, C. Depcik, A. Duncan, J. Guo, M. Mangus, E. Peltier, S. Stagg-Williams, Y.

Zhong, Investigation of the effects of biodiesel feedstock on the performance and emissions of a single-cylinder diesel engine, Energy and Fuels. 26 (2012) 2331–2341.

[33] P. Zhao, G. Li, Y. Yu, Numerical simulation and experimental study of heat and mass transfer in fuel droplet evaporation, Heat Mass Transf. 50 (2014) 1145–1154.

[34] H.-H. Chiu, T.M. Liu, Group Combustion of Liquid Droplets, Combust. Sci. Technol. 17 (1977) 127–142.

List of Figures

List of Tables

Combustion and Emission Performances of Coconut, Palm and Soybean Methyl Esters under Reacting Spray Flame Conditions

Meng Choung Chiong[a], Cheng Tung Chong[a,b,*], Jo-Han Ng[b,c,d], Manh-Vu Tran[e], Su Shiung Lam[f], Agustin Valera-Medina[g], Mohammad Nazri Mohd Jaafar[a]

[a] Faculty of Mechanical Engineering, Universiti Teknologi Malaysia, 81310 Skudai, Johor, Malaysia.
[b] UTM Centre for Low Carbon Transport in Cooperation with Imperial College London, Universiti Teknologi Malaysia, 81310 Skudai, Johor, Malaysia.
[c] Faculty of Engineering and The Environment, University of Southampton Malaysia, 79200 Iskandar Puteri, Johor, Malaysia.
[d] Energy Technology Research Group, Engineering Sciences, University of Southampton, SO17 1BJ, Hampshire, UK.
[e] School of Engineering, Monash University Malaysia, Jalan Lagoon Selatan, 47500 Bandar Sunway, Selangor, Malaysia.
[f] Eastern Corridor Renewable Energy Group (ECRE), Environmental Technology Programme, School of Ocean Engineering, Universiti Malaysia Terengganu, 21030 Kuala Terengganu, Terengganu, Malaysia.
[g] College of Physical Sciences and Engineering, Cardiff University, Wales, United Kingdom.

Abstract

The spray combustion characteristics of coconut (CME), palm (PME) and soybean (SME) biodiesels/methyl esters were compared with diesel by using an axial swirl flame burner. Atomisation of the liquid fuels was achieved via an airblast-type nozzle with varied atomising air-to-liquid ratios (ALR) of 2-2.5. The fully developed sprays were mixed with strongly swirled air to form combustible mixtures prior to igniting at the burner outlet. Under fuel-lean condition, biodiesel spray flames exhibited bluish flame core without the yellowish sooty flame brush, indicating low sooting tendency as compared to baseline diesel. Increasing the atomising air led to the reduction of flame length but increase in flame intensity. Measurements of post-combustion emissions show that SME produced higher NO as compared to CME and PME due to higher degree of unsaturation, while the most saturated CME showed the lowest NO and CO emissions amongst the biodiesels tested across all equivalence ratios. By preheating the main swirl air to 250 ^{o}C, higher emissions of NO, CO and CO_2 were observed for biodiesels. Higher ALR led to reduced NO and CO emissions regardless of the fuel used, making it a viable strategy to resolve the simultaneous NO-CO reduction conundrum. This work shows that despite different emission characteristics exhibited by biodiesels produced from different feedstock, they are in principle potential supplemental fuels for practical combustion systems. The higher pollutant emitted can be mitigated by operating at higher ALR in a twin-fluid based swirl combustor.

Keywords: Biodiesel; Soy; Palm; Coconut; Spray flame; Emissions

*Corresponding author
Address: Faculty of Mechanical Engineering, Universiti Teknologi Malaysia 81310 Skudai Johor, Malaysia.
Email: ctchong@mail.fkm.utm.my ; Phone: +60(7) 5534631 ; Fax: +60 (7) 5566159

1. Introduction

The recent energy outlook report by the International Energy Agency (IEA) has projected the energy dependent on biodiesels to grow from 0.83 EJ in 2015 to 5.97 EJ by the year 2035 [1]. The growing importance of biodiesel stems from the global decarbonising efforts, as the renewable fuel forms a closed-carbon cycle as opposed to the open-carbon cycle when utilising petroleum diesel [2]. Additionally, the use of biodiesel in combustion applications is comparatively cleaner than that of fossil diesel in terms of lower particulate matter (PM), sulphur dioxide (SO_2) and unburnt hydrocarbon (UHC) emissions [3,4]. While there are other alternative fuels that are also cleaner than fossil diesel in combustion application, biodiesel stands in the forefront as it can use existing diesel infrastructures and distribution channels [5]. This is due to its similar caloric value, viscosity and cetane number with diesel [6,7]. This has led to the widespread interest of applying biodiesel in reciprocating combustion engine for the transportation sector [8–10].

Fuel-flexible gas turbine is envisaged from the standpoint of reducing operating cost, while also meeting emissions targets. Biodiesel has been identified as one of the prospective alternative fuels for gas turbines. Biodiesel-fuelled gas turbines have been experimentally studied using lab-based swirl flame burners or actual gas turbine engines. A study on the spray and combustion properties of rapeseed biodiesel using a gas turbine-type burner concluded that, biodiesel spray exhibited longer spray penetration length and smaller spray cone angle as compared to that of diesel [11]. The phenomena are attributed to the higher density, viscosity, surface tension and boiling point of biodiesel as compared to that of conventional diesel fuel. It has also been found that biodiesel produced lower NO_x (nitrogen oxides) emissions by 21% when compared to that of diesel at an axial distance of 60 mm from the nozzle. This suggested that spray atomisation plays an important role in NO_x emissions. In another study using gas turbine swirl flame burner, it was again demonstrated that higher atomisation pressure resulted

in finer spray with smaller droplet size and subsequently lower NO_x emissions [12]. The NO_x emissions level was decreased from 13 ppm to 9 ppm as atomising pressure was increased from 0.4 to 0.8 MPa. The increase in droplet size causes larger number of droplets to be transported downstream of the flame, thus requiring longer evaporation time. Consequently, the ratio of combustion in diffusion mode to premixed mode increases, leading to greater incidences of the local regions with high temperatures, in turn causing greater amount of NO_x formed [12,13].

In a study that examined rapeseed biodiesel with swirl flame burner, it was demonstrated that rapeseed biodiesel's nitric oxide (NO) emissions were reduced by approximately 22% as compared to that of diesel, at 6 kW output power. It was postulated that the higher heat of vaporisation of the biodiesel spray and the presence of oxygen in the fuel may partially suppress the prompt NO formation mechanism [14]. In other related studies, carbon monoxide (CO) emission for biodiesel derived from soybean was reported to reduce by 50% as compared to that of diesel under fuel-mass specific by using a swirl burner equipped with an airblast type atomiser [15]. By utilising a flow blurring injector, it was demonstrated that mixing was improved and CO emissions of biodiesel flame could be reduced by 2-3 times when ALR was varied from 2.0 to 2.4 [16].

Applications of biodiesel in micro gas turbine (MGT) have been conducted by several other groups. In a study using a Capstone C30 MGT, soybean biodiesel was reported to cut down NO_x emissions by 60% as compared to that of fossil diesel [17]. However, in another study that utilised the same MGT model, soybean biodiesel was found to produce higher NO_x against that of diesel [18]. The higher NO_x emission from biodiesel was attributed to the larger biodiesel droplet size that led to the longer evaporation time scale that promotes NO_x emission [18]. In addition, the performances of soybean, canola, recycled rapeseed biodiesel and hog-fat biofuel against Jet A fuel were also investigated using a 30 kW gas turbine engine [19]. It was found that NO emissions for biodiesel were consistently lower than that of diesel for

equivalence ratio range of 0.15 to 0.30, with a maximum reduction of up to 75%, in spite of the similar turbine inlet and exhaust gas temperature for both biodiesel and diesel. Hence, it was postulated that NO_x formation in that instant was not dominated by thermal NO mechanism. CO emissions were found to be lower for biodiesels as the fuel-bound oxygen in the biodiesel assists in converting CO into CO_2 [19,20].

The thermal performance and emissions of a 30 kW MGT when fuelled with highly viscous castor biodiesel were compared with baseline diesel [21]. It was demonstrated that CO emission increased by 50% as compared to diesel at 14 kW engine output power, due to the inferior atomisation as a result of the high viscosity of castor biodiesel [21]. The authors also opined that the lower NO_x emissions achieved in the MGT tests are partly contributed by the same factor which results in lower combustion temperature. The size of castor biodiesel liquid droplets and primary-zone equivalence ratio are larger when compared with that of diesel. The reduction of temperature in the primary combustion zone (due to higher equivalence ratio) reduced the emission levels of the NO_x pollutants for biodiesel [21]. The emissions of 15% and 25% jatropha biodiesel-diesel blends were compared with neat diesel using a Rover gas turbine IS/60 test rig, where the blends showed higher emissions of NO_x by 34-42% as compared to that of diesel at the same power output [20]. It was postulated that the higher oxygen content in biodiesel led to higher flame temperature and subsequently higher level of NO_x emissions [20].

Applications of biodiesel in actual gas turbines have been conducted by several groups. The ignition, combustion dynamics and emissions of biodiesel in an industry gas turbine (Siemens SGT-100) were conducted by Liu et al. [22]. The NO_x emissions for biodiesel were found to be lower than that of diesel for all operating conditions tested. In another study, Moliere et al. [23] reported no smoke and sulphur oxide were emitted when the industrial gas

turbine (GE 6531B) was fuelled with biodiesel. These field tests indicate the positive effects of biodiesel towards the environment.

The variations in biodiesel feedstock, combustion chamber geometries, interaction between fuel spray and swirling air from the aforementioned studies have led to conflicting reports on the combustion and emissions characteristics of biodiesel usage in gas turbines. Additionally, most of the studies were conducted for the single feedstock biodiesel in isolation and without direct comparison against biodiesel from other feedstock within the same experimental studies.

Thus, this study adopts a multi-feedstock approach for an experimental investigation of biodiesel produced from coconut (CME), palm (PME) and soybean (SME) using a lab-based gas turbine type swirl burner operated at atmospheric condition. The study mainly investigates the effects of preheated air temperature, atomiser air-to-liquid (ALR) ratio, global equivalence ratio (ϕ) and degree of unsaturation level in biodiesels on the combustion and emissions characteristics of a model gas turbine swirl flame burner fitted with a twin-fluid nozzle. Fossil diesel is used as baseline fuel in this study.

2. Experimental setup

2.1 Operating fuels

The fuels used in this experimental study were coconut (CME), palm (PME) and soybean (SME) biodiesels, with fossil-based diesel as the baseline. Diesel was procured from a local gas station, while the tested biodiesels were produced from their respective vegetable oil counterparts in the lab via the transesterification process. The vegetable oils were reacted with methanol catalysed by potassium hydroxide (KOH) for 2 hours using a magnetic stirrer, with temperature maintained at 60 °C. The mass ratio of the vegetable oil:methanol:KOH was fixed at 113.75:50:1. Decanting was carried out to allow for the separation of reaction products

to remove glycerol and catalyst from the biodiesel. The produced biodiesel was then heated up to 120 °C for 4 hours to allow the evaporation of residual water and methanol.

A gas chromatograph (Agilent 7820A) was used to characterise the biodiesel. The composition for the CME, PME and SME produced are shown in Table 1. It can be observed that SME contains a substantial amount of unsaturated fatty acid with double bond at 83.87 wt%, while CME is mostly composed of saturated fatty acid with single bond at 92.82 wt%.

Physical properties for the tested fuels are shown in Table 2. Biodiesel is more viscous and less volatile as compared to diesel. The higher flash point of biodiesel results in lower volatility than diesel. Biodiesels also have lower calorific value of around 12.2-17.3% by mass, and 9.1-14.3% by volume as opposed to that of fossil diesel. This is due to the presence of fuel-bound oxygen content of in the range of 9.7-14.4% by weight for biodiesel.

2.2 Swirl Burner System

Fig. 1 illustrates the schematic diagram for the experimental setup. A gas turbine type swirl burner was used to establish a steady liquid spray flame. The axial swirler placed concentrically at the burner outlet consists of 6 straight vanes with the angle of 45°, forming the geometric swirl number of 0.84 based on Eq. 1 [24].

$$S_N = \frac{2}{3}\left[\frac{1-\left(D_h/D_s\right)^3}{1-\left(D_h/D_s\right)^2}\right]\tan\theta \tag{1}$$

where D_h and D_s are the diameters of the swirler hub and the swirler, respectively. The angle of the swirl blade from the centreline is denoted by θ. A swirling air flow that envelopes the atomised spray is formed when the main air passes through the swirler, forming a combustible

mixture. The swirler generates a high intensity recirculating flow to assist in fuel-air mixing and flame stabilisation.

The liquid fuel was delivered by a peristaltic pump (Longer BQ50-1J) and a flow damper was utilised to damp out the pulsating flow ripple caused by the peristaltic motion. Silicone tube with an inner diameter of 4 mm was used for the peristaltic pump to transfer the fuel. Prior to mixing with main swirling air, the fuel was atomised by a commercial twin-fluid atomiser (Delavan: SN type-30610-1). The atomising air and fuel orifice diameters are 1.73 and 0.50 mm, respectively. The supply of the atomising air and combustion air were controlled by air mass flow controllers (Sierra SmartTrak 50).

For the preheating of the main air, three rope heaters (Omega: FGR-100–240V) with a rated output of 500 W were used. The burner's plenum was insulated with heat resistant ceramic wool to minimise heat loss. A 1.5 mm K-type thermocouple was placed 10 mm upstream of the burner to measure the temperature of the preheated main air flow. This thermocouple provides feedback to the Proportional-Integral-Derivative (PID) controller to regulate the heating process. Flue gas from the combustion was directed to the exhaust by a 400 mm long, 130 mm diameter flame tube made from carbon steel, as depicted in Fig. 1.

2.3 Measurement techniques

2.3.1 Flame Imaging

A Canon EOS 600D digital camera was utilised to acquire the global flame images through a quartz wall that is optically accessible. Focal length and exposure time of 4 mm and 1/15 s, respectively, were used to capture the flame images.

2.3.2 Gas analyser

A gas analyser (KANE; KM9106 Quintox) was used to measure the concentrations of post-combustion NO, CO and CO_2 products in the flue gas at the outlet of combustor. The sampling was carried out by placing the probe 13 mm inward from the combustor exit. Emissions were measured at 5 spatial locations that were radially and equally spaced. Calibration gases were used to check the accuracy of the gas analyser before measurements. The sampling probe is 5 mm in diameter and the gas analyser sampled the flue gas at the rate of 2 L/min. The NO and CO emissions were measured via chemical sensors in the gas analyser, while the CO_2 emissions were calculated based on the measured oxygen (O_2). The probe sampled for 90 seconds at each spatial location to ensure steady state readings. The final global emissions for each test case were obtained by averaging the spatial readings using the area-weighted averaging method. The measurement range, resolution and propagated error for NO, CO, CO_2 and O_2 are summarised in Table 3.

2.4 Operating conditions

The liquid fuels and atomising air were independently delivered to the burner outlet at room temperature. The main combustion air was preheated to 250 °C prior to its mixing with the liquid fuel spray. Fuel flow rate was adjusted for each fuel to achieve a fixed power output of 9.3 kW. The atomisation air-to-liquid ratio (ALR) was varied at 2.00, 2.25 and 2.50 by regulating the flow rate of atomising air while holding the fuel flow rate constant. The ALR of 2.00 was chosen as the lower limit as it is near the limit of ALR where atomising air is adequate to produce proper spray [26]. For each of the ALR, the equivalence ratio was varied from 0.65 to 0.90 to simulate lean combustion regime in gas turbine. The mass flow rates for combustion air and fuel at equivalence ratio 0.65 are shown in Table 4 for different fuels.

3. Results and Discussion

3.1 Reacting Spray Imaging

The flame appearances for diesel, PME, SME and CME established at ALR=2.50 for equivalence ratios of $\phi = 0.90$ and 0.65 are shown in Fig. 2. It is shown that downstream region of the diesel main reaction zone is occupied by a distinct orange-yellow luminous flame, while biodiesels show mainly bluish flames. The orange-yellow luminous flame is due to the burning of soot particles in this region. Soot consists of aromatic structure, therefore fuels that contain substantial amount of aromatics structure in its chemical composition, such as diesel, is expected to be sootier than those from biodiesels [27]. Soot production was shown to increase linearly with increasing aromatic contents in the fuel [27]. On the other end, bluish flame at the verge of nozzle outlet is equivalent to the premixed flame caused by internal mixing between the atomising air and fuel. The presence of bulk oxygen increases oxidation rate of soot particles, resulting in reduced luminous orange-yellow sooty flame [28].

In contrast to diesel, biodiesels show distinctively different spray flame appearance with the notable absence of sooty orange at their post-reaction zones for the higher ALR cases. The absence of aromatics structure in biodiesels also greatly reduces the soot formation tendencies in biodiesels, due to the lack of the soot precursors. The fuel-bound oxygen content for the fatty acid methyl ester molecules also promotes soot oxidation, which is another reason for lower soot production in biodiesel spray flames [28]. By reducing the ALR to 2.0, inferior atomisation results in poorer mixing between reactants and air. This consequently incurs substantial soot formation due to incomplete combustion. The increase of soot formation at lower ALR is shown in Fig. 3 by the distinctively larger orange-yellow flame brush for all fuels.

Apart from the fuel properties, the dynamics of the flow also affects the flame appearance. A notable structure in a typical swirl stabilised flame is the presence of central toroidal recirculation zone (CTRZ) [29]. CTRZ plays essential role in stabilising the flame as

it recirculates the hot flue gas back into the reaction zone to constantly heat up the reactants. The presence of CTRZ directs the fuel spray towards the radial direction, forming a dual shear layer. The shear layer is the region where mixing and reaction of the reactant and oxidiser take place [29]. The presence of dual shear layer is notable for biodiesels spray flame. For diesel, however, the appearance of shear layer is overshadowed by the sooty orange-yellow flame. At lower equivalence ratio, greater amount of air flow generates a more concentrated CTRZ that subsequently moved the stagnation point towards upstream position to form a heart-shape reaction flame core.

3.2 Post-combustion Emissions

3.2.1 Effect of Main Swirl Air Temperature

The emissions of NO as a function of equivalence ratio at elevated main air temperature of 30 and 250 °C are shown in Fig. 4. Higher level of NO emission was shown for all fuels tested at elevated main air temperature. The energy provided from the preheated air assists the species molecules to surpass the energy threshold easier for chemical reactions, thus enabling greater amount of energy release with higher flame temperature that subsequently leads to higher NO [30]. Fuel wise, biodiesels exhibit generally higher NO emission as compared to that of diesel for both 250 ^{o}C and 30 ^{o}C main air temperatures. The main exception would be the highly saturated CME. This is postulated to be due to biodiesels possessing larger droplets size and lower volatility as compared to diesel, leading to longer droplets residence time [24]. Longer droplets residence time subsequently promotes thermal NO formation. Apart from thermal NO, prompt NO constitutes another portion of NO emission. The formation of prompt NO depends very much on methylidyne (CH) radical, which serves as the precursor for prompt NO formation [30]. It was shown that biodiesels produced more CH radical than diesel, which

inherently elevates prompt NO formation as compared to diesel [30,31]. The elevation of both thermal and prompt NO result in higher NO emission for biodiesel as compared to diesel.

It can be observed that SME produced the highest NO, followed by PME and CME for the preheated main air temperature cases at ALR = 2.5 and power output of 9.3 kW. The trend of NO emission was found to correlate with unsaturation degree of the biodiesels, where highly unsaturated biodiesel (SME) produces more NO emissions as compared to that of the saturated biodiesel (CME). This is in due to the double bond in unsaturated biodiesel that releases more energy when breaking up as compared to single bond, thus inherently increased adiabatic flame temperature and thermal NO formation [32]. In addition, highly unsaturated biodiesels also promote the formation of CH radicals that serve as the precursor for prompt NO formation, which is another reason that contributes to higher NO emissions [31]. Such trends were not observed for the non-heated main air flow cases where PME produced greater NO emissions than that of the more unsaturated SME.

The CO emissions from biodiesels were generally higher than that of diesel throughout the equivalence ratios investigated for both non-heated and preheated main air conditions, as shown in Fig. 5. Larger fuel droplets and lower fuel volatility of biodiesel inhibit complete combustion, which consequently results in greater CO emission as compared to that of diesel. SME and PME that possess higher viscosity and lower volatility result in higher CO emission as compared to CME. This is due to the higher viscosity and lower fuel volatility slowing down droplet vaporisation rate, subsequently hindering the complete combustion process. At higher preheating temperature, the CO emission level is lower than non-heated case by approximately a factor of 2, which is a reverse trend of NO (Fig. 4). This is expected as preheated air promotes higher efficiency in combustion with higher flame temperature that increases NO but lowering the CO.

The effect of equivalence ratio on the NO and CO emissions are elucidated in Fig. 4 and Fig. 5, respectively. At $\phi = 0.9$, the relatively lower main air flow reduces the turbulence intensity that consequently weakens the CTRZ. This causes poorer mixing and increases the CO emission. As more air is introduced, the overall mixture equivalence ratio is reduced, hence strengthening the CTRZ due to increased swirl intensity that promotes the mixing between the reactants and oxidiser. A more complete combustion is achieved whereas CO emission is reduced substantially. Minimum CO typically occurs at equivalence ratios between 0.7 and 0.8.

Increasing the main air further generates an even stronger CTRZ that recirculates post combustion products back to the flame root. As a consequent, a lower temperature region is formed around the central region of the flame that is in contact with the recirculated gases [29]. The rate of chemical reaction is suppressed in this region due to the lower temperature. CTRZ now weakens the chemical reaction rate instead of promoting the combustion, as indicated by slight CO increment below $\phi = 0.7$. As shown in Fig. 4, maximum NO is produced within the equivalence ratio range, where minimum CO is produced for all fuels. It is hence observable that NO-CO has a distinct trade-off relationship.

The effect of main air temperature on CO_2 emissions is shown in Fig. 6 for diesel and biodiesels. Overall, elevating the main air temperature leads to increase of CO_2 emissions, as a result of increased flame temperature and enhanced CO oxidation rate into CO_2. [30]. As the fuel/air mixture approaches stoichiometric condition, CO_2 concentration increases due to conversion of more carbon from the fuel into CO_2. Higher CO_2 was shown by biodiesels as compared to diesel, partly in due to the increased mass flow rate of fuel to compensate for the lower energy density, as more carbon on a mass basis from the heavier biodiesel chain contributes to the formation of CO_2 during reaction. Among the biodiesels, the unsaturated SME shows higher CO_2 emissions as compared to PME and CME, similar to the trend of NO emissions.

3.2.2 Effect of Air-Liquid Ratio (ALR)

Variation of the ALR imposes significant effects on the emissions. The NO emission is reduced by up to a factor of 2 for the three biodiesels when the ALR is increased from 2.0 to 2.5, as shown in Fig. 7a. The reduction of NO emissions for diesel is less pronounced than those from biodiesel fuels. At lower ALR, inadequate supply of atomising air results in inferior atomisation due to relatively low momentum of air in breaking up the spray. Formation of dense fuel-rich mixture in the spray core inhibits effective heat transfer to the droplets [33]. Fuel droplets that are not fully vaporised are dispersed away by the surrounding air flow. As a consequent, flammable mixture is formed at some distance away from the spray periphery, causing it to burn in diffusional mode which leads to the increase of local flame temperature that promotes thermal NO formation [30]. Conversely, at higher ALR, strong atomising air momentum imparted on the liquid jet produces fine droplets. The sparsely distributed droplets allow greater amount of oxygen to penetrate into the drops cloud [34], where the turbulent flow subsequently accelerates droplet vaporisation rate [33].

A uniform reduction trend of CO emission for all fuels tested was seen with increasing ALR as shown in Fig. 7b. At lower ALR, inferior atomisation forms dense fuel-rich spray with minimum oxygen penetration, causing locally fuel-rich combustion due to the lack of oxygen for complete combustion, thus leading to the increase of CO formation. Fig. 7c shows that CO_2 concentration tends to be slightly higher at ALR=2.0 as compared to ALR=2.5. This could be due to higher combustion temperature at ALR=2.0 that accelerates the oxidation rate from CO into CO_2 [30]. The higher O_2 at ALR=2.5 (Fig. 7d) contributes to the lower NO as lower flame temperature is attained at the spray centreline region. Better mixing was achieved at ALR=2.5 that contributes to the reduction of CO as more efficient combustion is enabled.

339 Interestingly, biodiesels exhibit higher NO, CO and CO_2 than baseline diesels at all
340 ALR tested, which corroborates with the results shown in previous section. SME shows higher
341 NO, CO and CO_2 among all biodiesels, indicating the effect of unsaturation in the molecule is
342 evident during reaction. CME shows the lowest NO and CO emissions among biodiesels but
343 still displaying higher amount than that of baseline diesel. Despite the higher emissions
344 characteristics for biodiesels, increasing the ALR is an effective way of reducing NO and CO
345 to the level comparable to diesel.
346

347 **4. Conclusion**

348 In this experimental study, the emission characteristics of PME, SME and CME were
349 compared against that of fossil diesel under the same output flame power of 9.3 kW. The main
350 findings from the study are:

351 a. diesel flame shows a distinct luminous orange-yellow flame at the downstream of the
352 main reaction zone, whereas all of the biodiesels tested show mainly bluish flames. The
353 luminous orange-yellow flame indicates the presence of soot in the diesel spray flame,
354 which is almost absent in biodiesel spray flames.
355 b. by increasing the main air temperature, chemical reaction rate accelerates and
356 subsequently increases the production of NO. Conversely, CO emission is reduced due
357 to incomplete combustion.
358 c. comparison of the NO emission profiles shows that biodiesels produce higher NO
359 compared to diesel. The NO formation in biodiesel is due to higher adiabatic flame
360 temperatures and prolonged droplet residence time that give rise to the thermal NO
361 formation.

d. NO and CO emissions comparison among the three biodiesels shows that highly unsaturated biodiesel (SME) exhibits higher NO production tendency than saturated biodiesel (CME).

e. from a physical property perspective, biodiesel with higher viscosity and lower fuel volatility such as SME produces greater amount of CO as compared to that of CME.

f. a clear trade-off characteristic between NO-CO can clearly be observed when varied against equivalence ratio at a fixed ALR and air temperature.

g. by varying the ALR, the emission profiles are altered, whereby an increase of ALR leads to the simultaneous reduction of NO, CO and CO_2. The study shows that atomisation method and fuel properties directly influence the combustion behaviour, which consequently affects the formation rate of final emissions products.

h. biodiesels have been shown to be suitable supplemental fuels in combustion systems that employ swirl flames such as gas turbines, furnaces and boilers. The higher emissions of biodiesels can be effectively mitigated by utilising the strategy of higher ALR in a twin-fluid atomiser based combustor.

Acknowledgement

Financial support from the Malaysian Ministry of Higher Education and Universiti Teknologi Malaysia (Research University Flagship Grant vote no. 03G63) is gratefully acknowledged.

References

[1] IEA, Technology Roadmap: Delivering Sustainable Bioenergy, 2017.

[2] J.H. Ng, H.K. Ng, S. Gan, Recent trends in policies, socioeconomy and future directions of the biodiesel industry, Clean Technol. Environ. Policy. 12 (2010) 213–238.

[3] V. Soloiu, M. Dunggan, S. Harp, B. Vlcek, D. Williams, PFI (port fuel injection) of n-butanol and direct injection of biodiesel to attain LTC (low temperature combustion) for low-emissions idlingin a compression engine, Energy. 52 (2013) 143–154.

[4] V. Soloiu, J.D. Moncada, R. Gaubert, M. Muiños, S. Harp, M. Ilie, A. Zdanowicz, G. Molina, LTC (low-temperature combustion) analysis of PCCI (premixed charge compression ignition) with n-butanol and cotton seed biodiesel versus combustion and emissions characteristics of their binary mixtures, Renew. Energy. 123 (2018) 323–333.

[5] M. Çetinkaya, Y. Ulusoy, Y. Tekìn, F. Karaosmano□lu, Engine and winter road test performances of used cooking oil originated biodiesel, Energy Convers. Manag. 46 (2005) 1279–1291.

[6] R. Alloune, M. Balistrou, S. Awad, K. Loubar, M. Tazerout, Performance, combustion and exhaust emissions characteristics investigation using Citrullus colocynthis L. biodiesel in DI diesel engine, J. Energy Inst. 91 (2016) 434–444.

[7] J. Thangaraja, K. Anand, P.S. Mehta, Biodiesel NOx penalty and control measures - A review, Renew. Sustain. Energy Rev. 61 (2016) 1–24.

[8] C.T. Chong, J.-H. Ng, S. Ahmad, S. Rajoo, Oxygenated palm biodiesel: Ignition, combustion and emissions quantification in a light-duty diesel engine, Energy Convers. Manag. 101 (2015) 317–325.

[9] H. Chen, Q. Guo, X. yi Zhao, M. long Xu, Y. Ma, Influence of fuel temperature on combustion and emission of biodiesel, J. Energy Inst. 89 (2016) 231–239.

[10] H. Chen, J. He, Y. Chen, H. Hua, Performance of a common rail diesel engine using biodiesel of waste cooking oil and gasoline blend, J. Energy Inst. (2017) 1–11.

[11] L. Li, X. Zhang, Z. Wu, J. Deng, C. Huang, Experimental study of biodiesel spray and combustion characteristics, Powertrain Fluid Syst. Conf. Exhib. (2006).

[12] N. Hashimoto, Y. Ozawa, N. Mori, I. Yuri, T. Hisamatsu, Fundamental combustion characteristics of palm methyl ester (PME) as alternative fuel for gas turbines, Fuel. 87 (2008) 3373–3378.

[13] H. V. Panchasara, B.M. Simmons, A.K. Agrawal, S.K. Spear, D.T. Daly, Combustion Performance of Biodiesel and Diesel-Vegetable Oil Blends in a Simulated Gas Turbine Burner, J. Eng. Gas Turbines Power. 131 (2009) 31503.

[14] C.T. Chong, S. Hochgreb, Flame structure, spectroscopy and emissions quantification of rapeseed biodiesel under model gas turbine conditions, Appl. Energy. 185 (2017) 1383–1392.

[15] D. Sequera, A.K. Agrawal, S.K. Spear, D.T. Daly, Combustion Performance of Liquid Biofuels in a Swirl-Stabilized Burner, J. Eng. Gas Turbines Power. 130 (2008) 32810.

[16] B.M. Simmons, A.K. Agrawal, Combustion Science and Technology Flow Blurring Atomization for Low- Emission Combustion of Liquid Biofuels, Combust. Sci. Technol. 184 (2012) 660–675.

[17] C.R. Krishna, Performance of the Capstone C30 Microturbine on Biodiesel Blends, (2007) 1–11.

[18] C.D. Bolszo, V.G. McDonell, Emissions optimization of a biodiesel fired gas turbine, Proc. Combust. Inst. 32 (2009) 2949–2956.

[19] Z. Habib, R. Parthasarathy, S. Gollahalli, Performance and emission characteristics of biofuel in a small-scale gas turbine engine, Appl. Energy. 87 (2010) 1701–1709.

[20] A. Rehman, D.R. Phalke, R. Pandey, Alternative fuel for gas turbine: Esterified jatropha oil-diesel blend, Renew. Energy. 36 (2011) 2635–2640.

[21] M.A.R. Nascimento, E.S. Lora, P.S.P. Corrêa, R. V. Andrade, M.A. Rendon, O.J. Venturini, G.A.S. Ramirez, Biodiesel fuel in diesel micro-turbine engines: Modelling and experimental evaluation, Energy. 33 (2008) 233–240.

[22] K. Liu, J.P. Wood, E.R. Buchanan, P. Martin, V.E. Sanderson, Biodiesel as an Alternative Fuel in Siemens Dry Low Emissions Combustors: Atmospheric and High Pressure Rig Testing, J. Eng. Gas Turbines Power. 132 (2010) 11501.

[23] M. Moliere, E. Panarotto, M. Aboujaib, J.M. Bisseaud, A. Campbell, J. Citeno, P.-A. Maire, L. Ducrest, Gas turbines in alternative fuel applications: Biodiesel field test, Proc. Asme Turbo Expo 2007, Vol 1. (2007) 397–406.

[24] C.T. Chong, S. Hochgreb, Spray combustion characteristics of palm biodiesel, Combust. Sci. Technol. 184 (2012) 1093–1107.

[25] S.K. Hoekman, A. Broch, C. Robbins, E. Ceniceros, M. Natarajan, Review of biodiesel composition, properties, and specifications, Renew. Sustain. Energy Rev. 16 (2012) 143–169.

[26] C.T. Chong, S. Hochgreb, Effect of Atomizing Air Flow on Spray Atomization of an Internal-Mix Twin-Fluid Atomizer, At. Sprays. 25 (2015) 657–673.

[27] F. Cignoli, S. De Iuliis, G. Zizak, Soot load versus aromatic concentration in diesel oil premixed flames, Fuel. 80 (2001) 945–955.

[28] W. Merchan-Merchan, S. McCollam, J.F.C. Pugliese, Soot formation in diffusion oxygen-enhanced biodiesel flames, Fuel. 156 (2015) 129–141.

[29] J. Kwark, Y. Jeong, C. Jeon, Effect of Swirl Intensity on the Flow and Combustion of a Turbulent Non-Premixed Flat Flame, Flow, Turbul. Combust. 73 (2004) 231–257.

[30] A.H. Lefebvre, D.R. Ballal, Gas Turbine Combustion: Alternative Fuels and Emissions, 3rd ed., CRC Press, 2010.

[31] B. Bazooyar, S.H. Hashemabadi, A. Shariati, NOx formation of biodiesel in utility power plant boilers; Part B. Comparison of NO between biodiesel and petrodiesel, Fuel. 182 (2016) 323–332.

[32] E. Cecrle, C. Depcik, A. Duncan, J. Guo, M. Mangus, E. Peltier, S. Stagg-Williams, Y.

Zhong, Investigation of the effects of biodiesel feedstock on the performance and emissions of a single-cylinder diesel engine, Energy and Fuels. 26 (2012) 2331–2341.

[33] P. Zhao, G. Li, Y. Yu, Numerical simulation and experimental study of heat and mass transfer in fuel droplet evaporation, Heat Mass Transf. 50 (2014) 1145–1154.

[34] H.-H. Chiu, T.M. Liu, Group Combustion of Liquid Droplets, Combust. Sci. Technol. 17 (1977) 127–142.

List of Figures

List of Tables

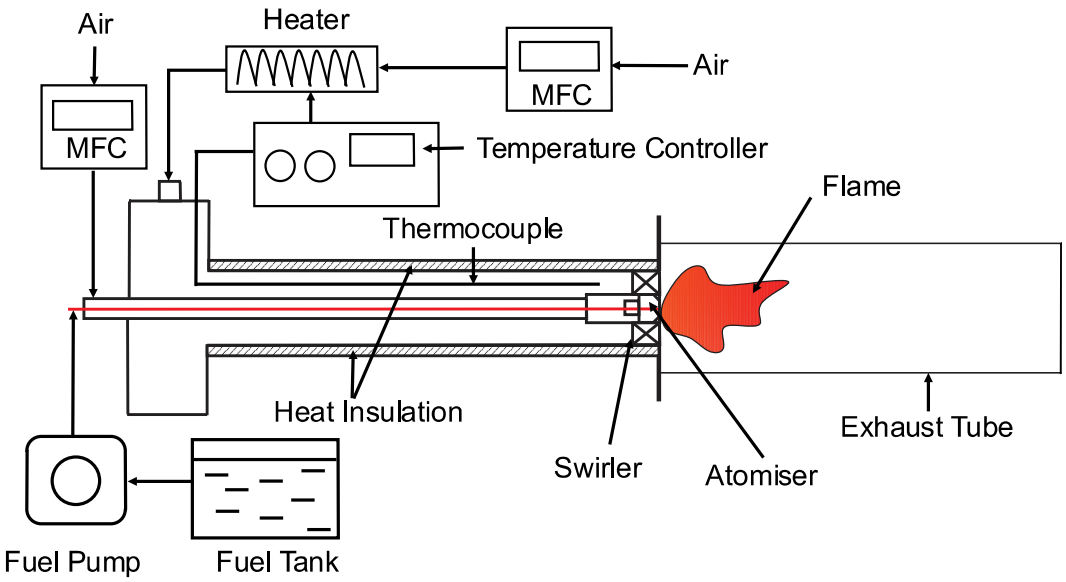

Fig. 1 Schematic diagram for reacting spray rig.

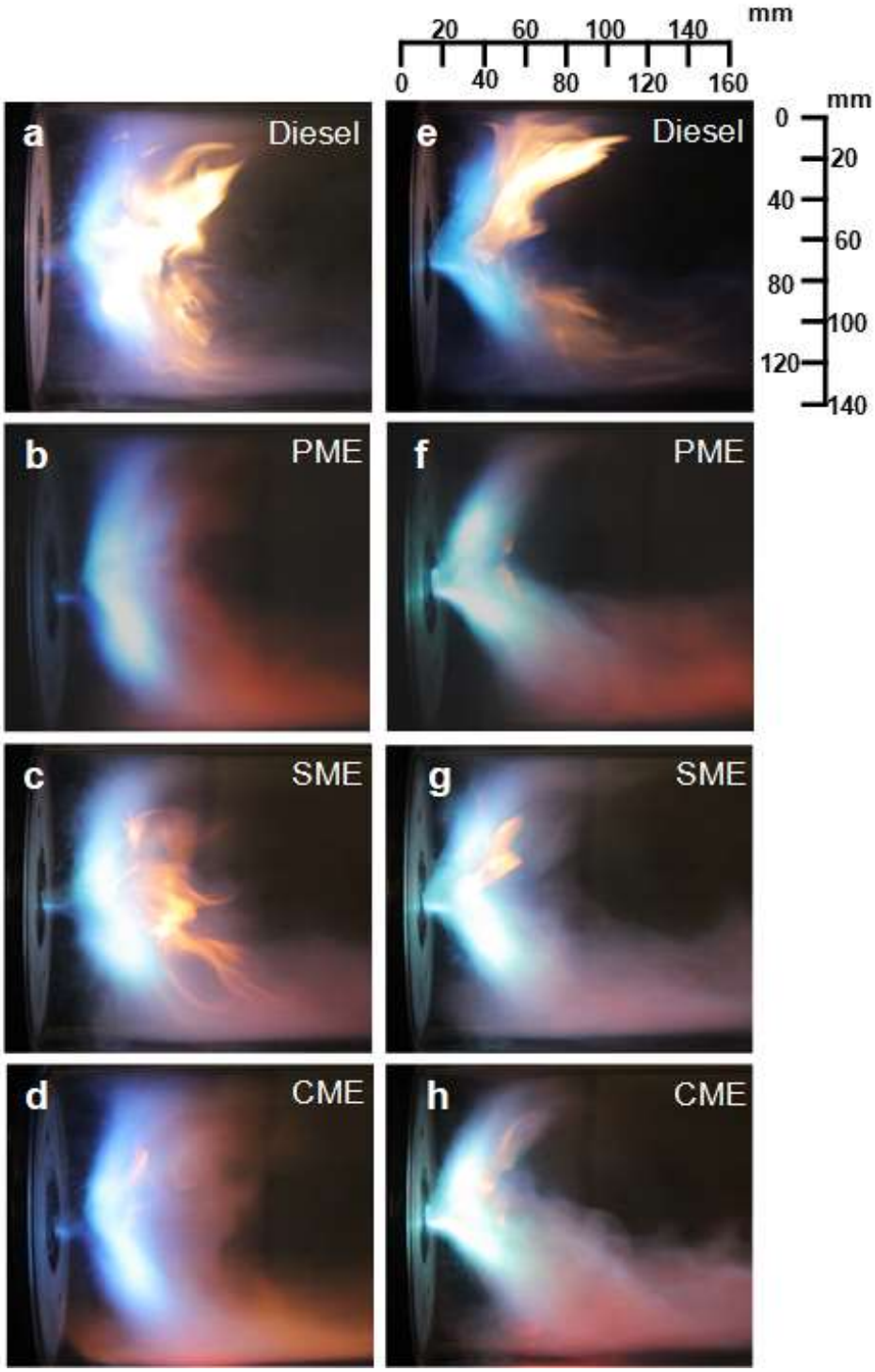

Fig. 2 Flame images for diesel, PME, SME and CME spray flames established at ALR=2.50, (a-d) $\phi = 0.90$ and (e-h) $\phi = 0.65$ and fixed power output of 9.3 kW.

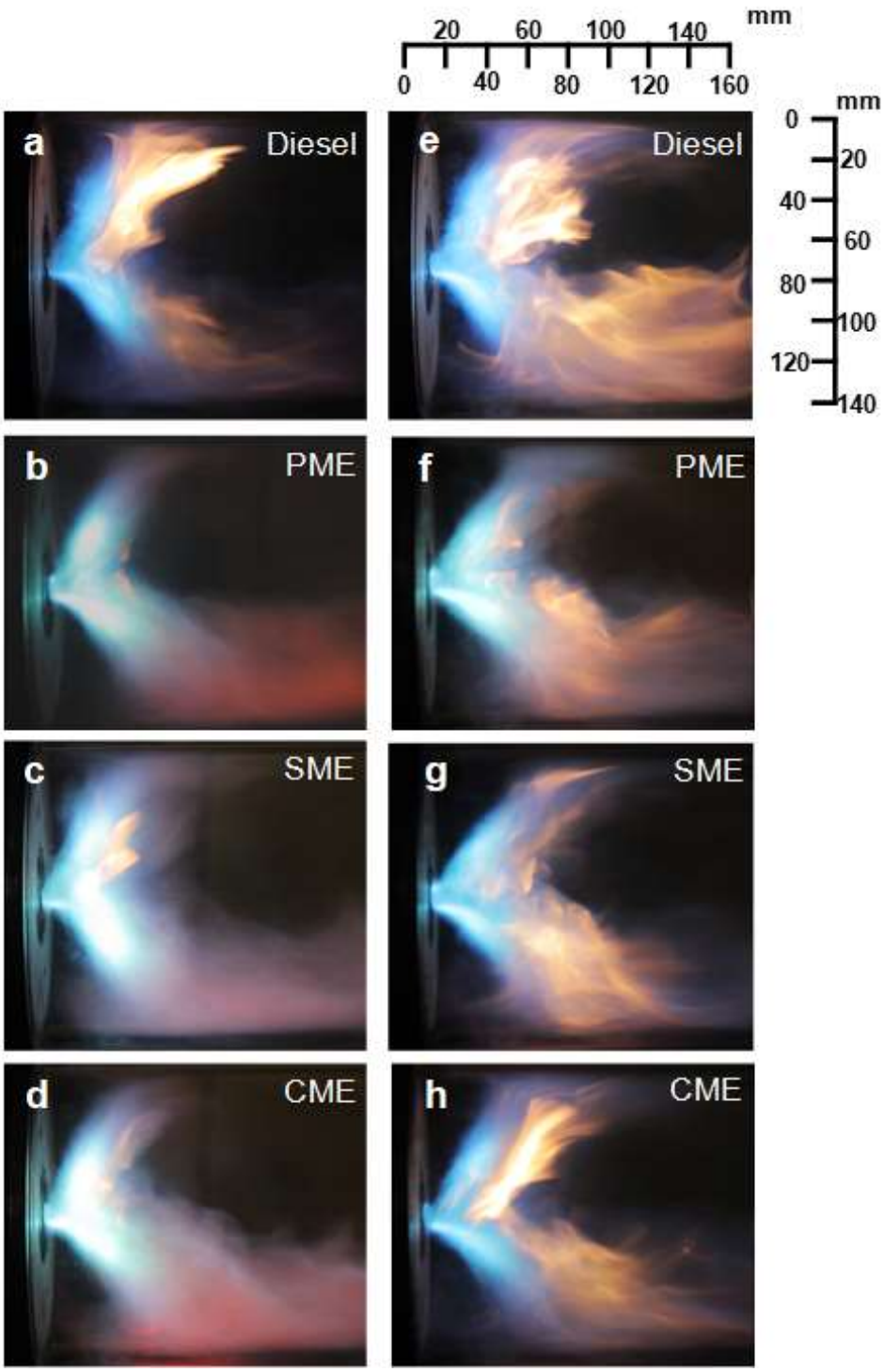

Fig. 3 Flame images for diesel, PME, SME and CME spray flames established at $\phi = 0.65$, (a-d) ALR = 2.50, (e-h) ALR = 2.0 and fixed power output of 9.3 kW.

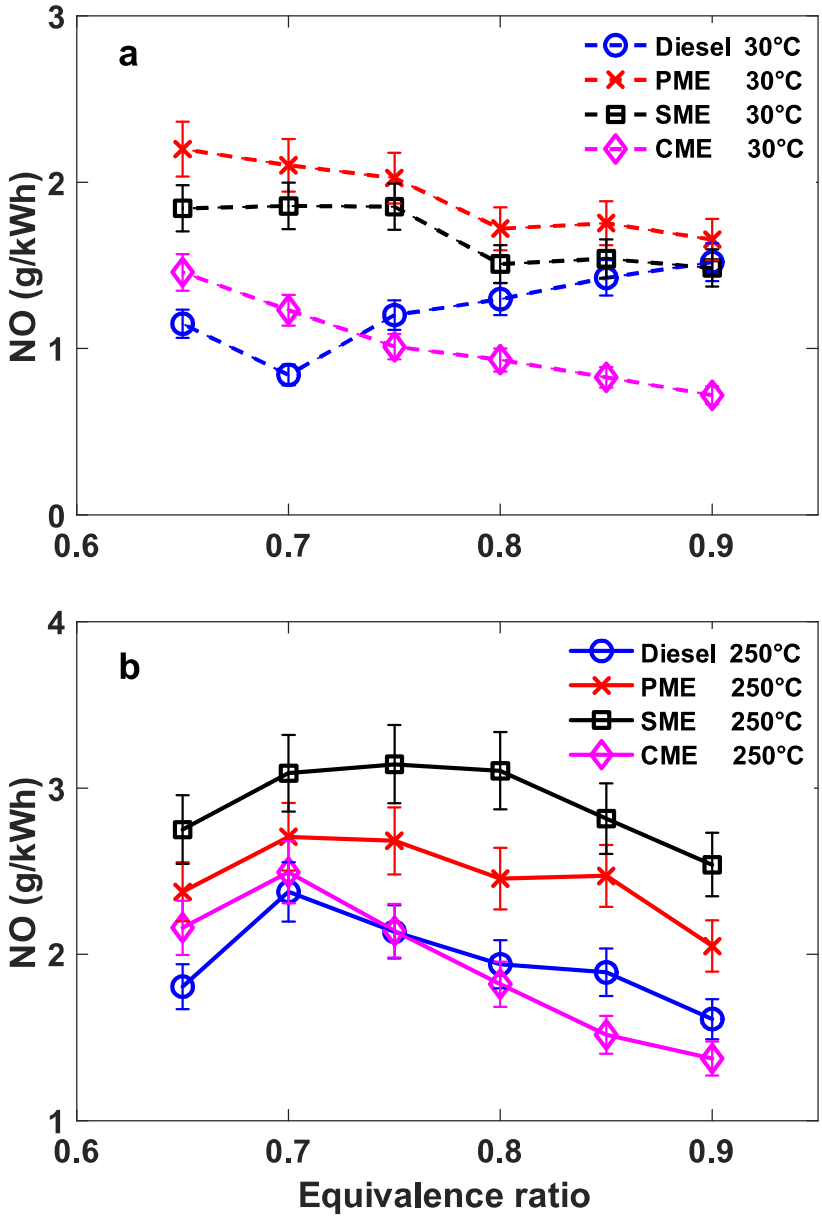

Fig. 4 NO emissions at varied equivalence ratios for diesel, PME, SME and CME at (a) 30 °C and (b) 250 °C, ALR= 2.5 and power output of 9.3 kW.

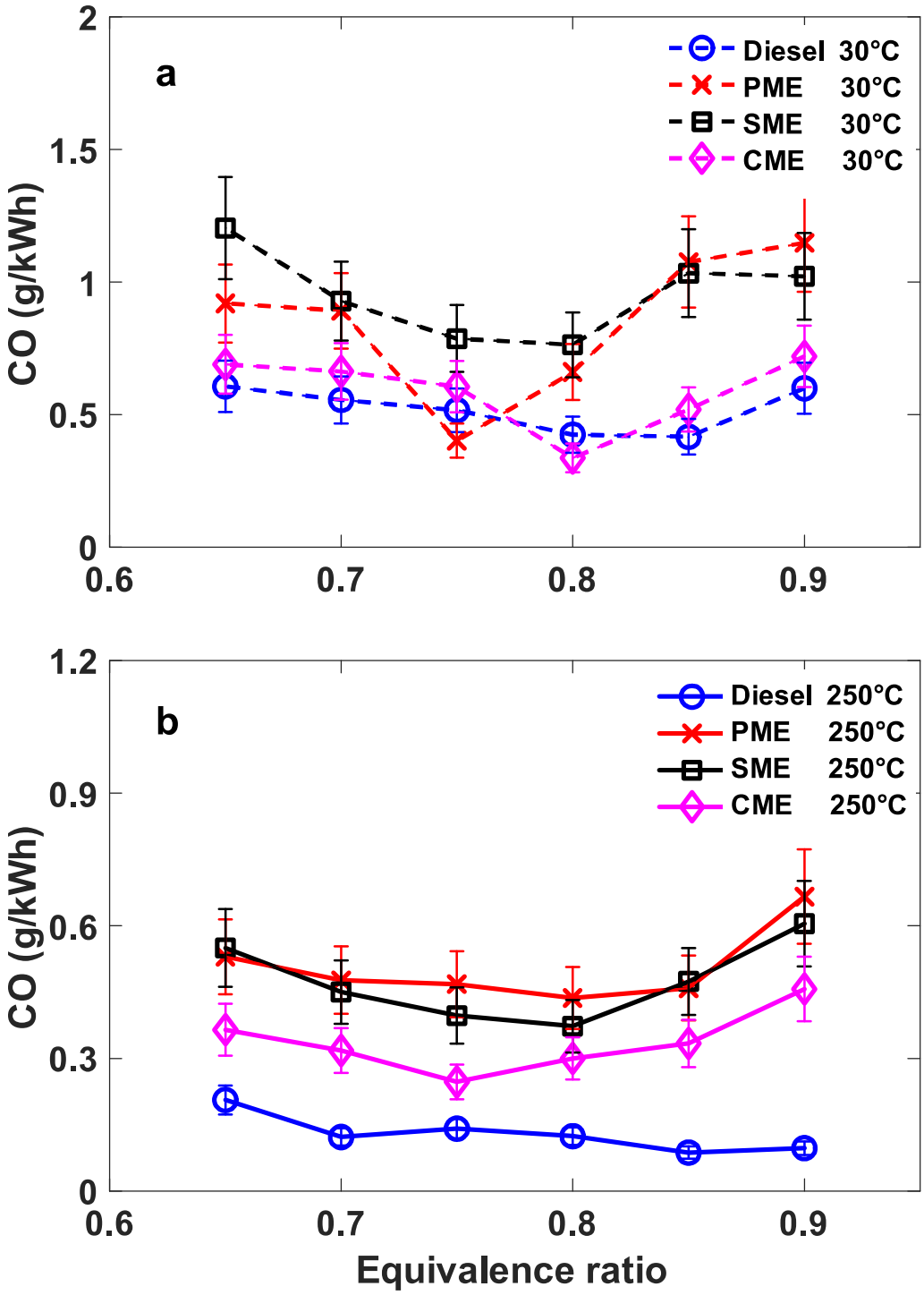

Fig. 5 CO emissions at varied equivalence ratio for diesel, PME, SME and CME at (a) 30 °C and (b) 250 °C, ALR= 2.5 and power output of 9.3 kW.

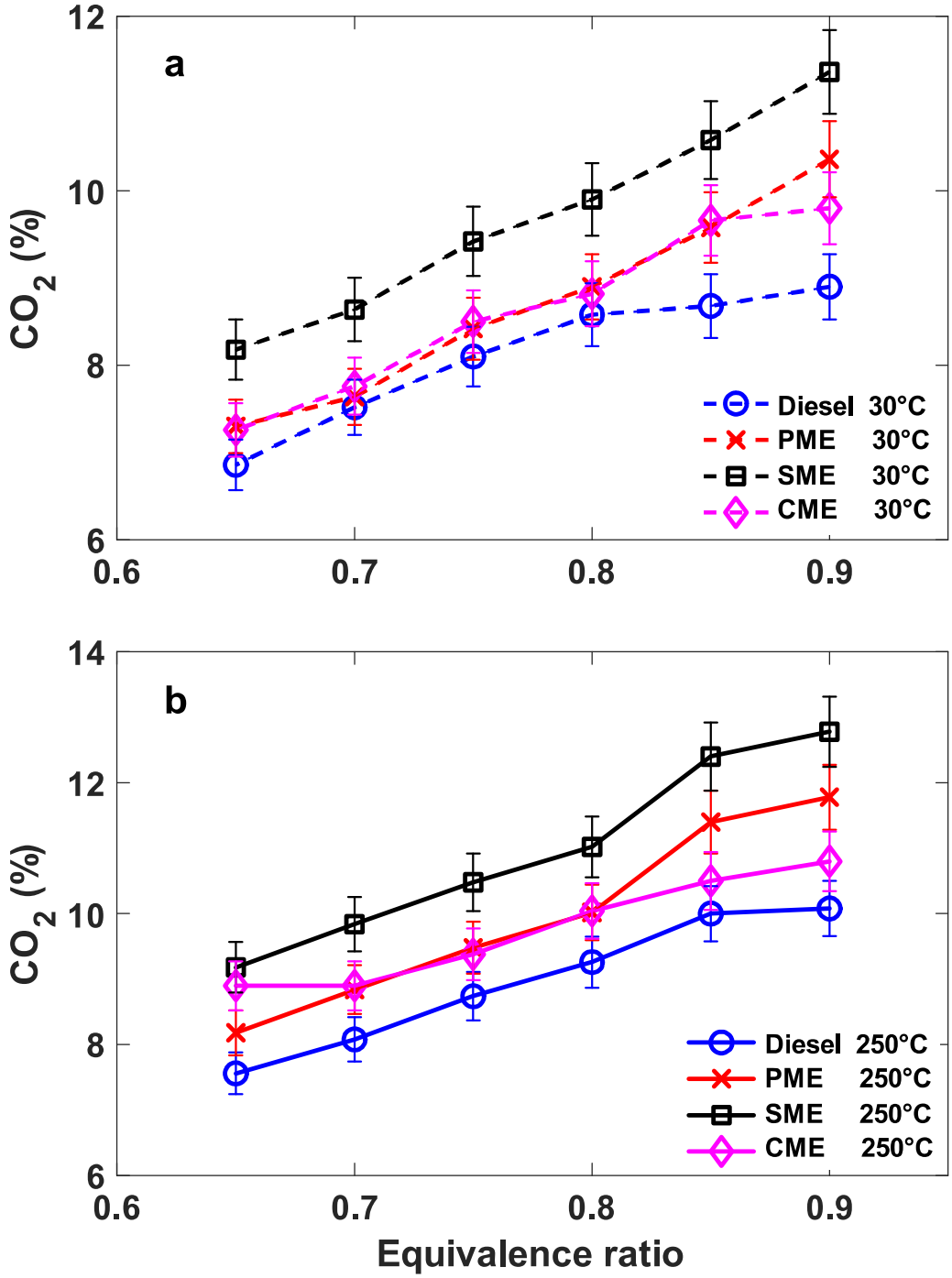

Fig. 6 CO_2 emissions as a function of equivalence ratio for diesel, PME, SME and CME at (a) 30 °C and (b) 250 °C, ALR= 2.5 and power output of 9.3 kW.

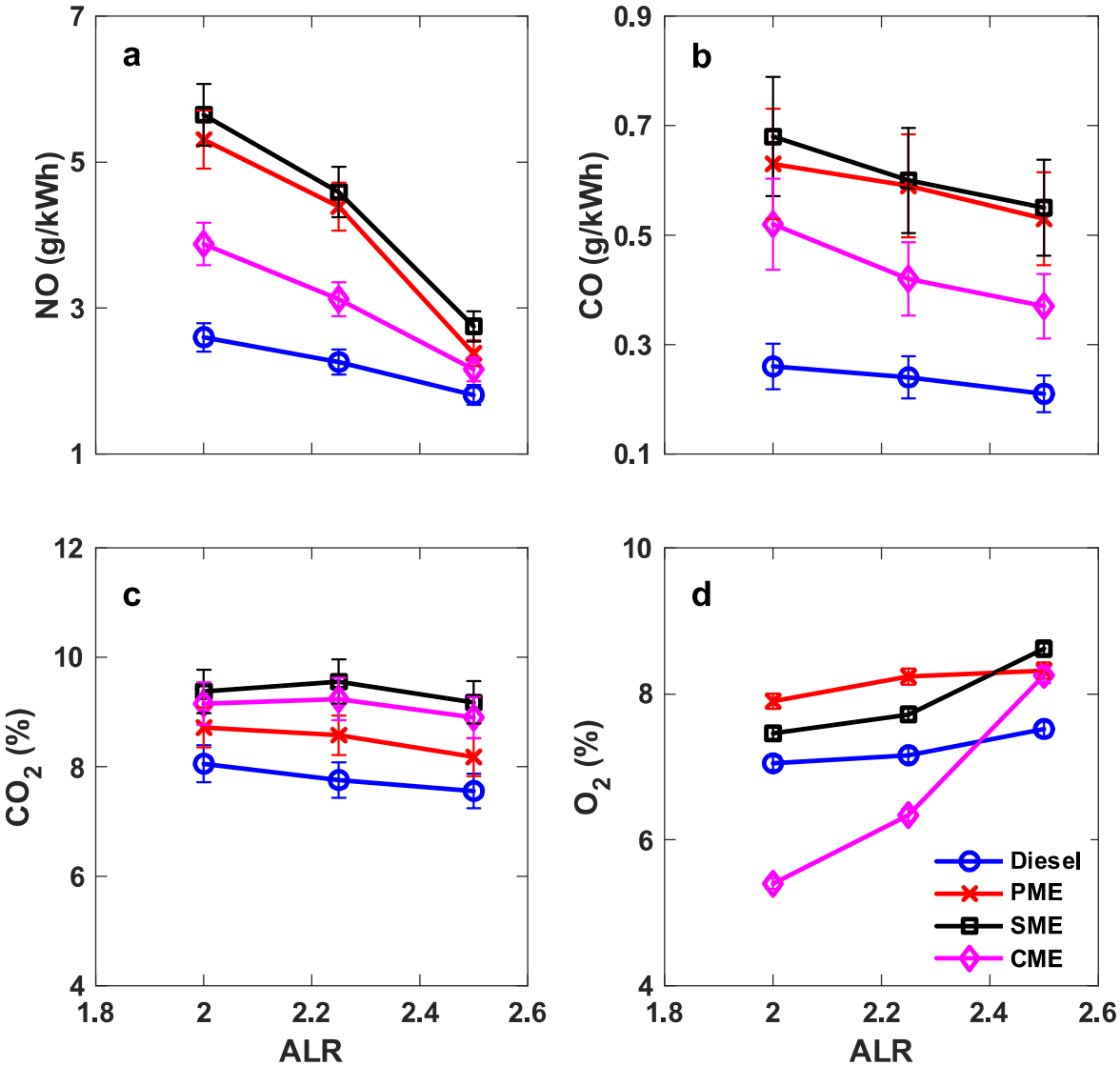

Fig. 7 Emissions of (a) NO, (b) CO, (c) CO_2 and (d) O_2 against ALR for diesel, PME, SME and CME at $\phi = 0.65$ and main air temperature of 250 ^{o}C.

Table 1 Composition by mass for CME, PME and SME

Fatty Acid	Structure	No of Carbon: double bond	Composition (wt%)		
			PME	SME	CME
Caprylic	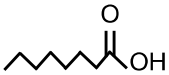	C8:0	-	-	6.78
Capric	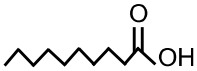	C10:0	-	-	5.61
Lauric		C12:0	-	-	51.00
Myristic		C14:0	0.93	-	18.51
Palmitic		C16:0	39.85	11.62	9.26
Stearic		C18:0	3.55	4.51	1.66
Oleic	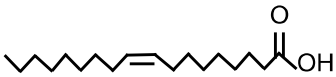	C18:1	43.14	23.03	6.06
Linoleic	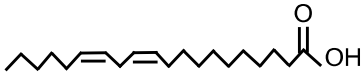	C18:2	12.53	54.22	1.12
Linolenic		C18:3	-	6.62	-

Table 2 Physical properties for diesel and biodiesels [24,25]

Properties	Unit	Diesel	PME	SME	CME
C	[% wt]	85.0	76.0	77.2	73.9
H	[% wt]	15.0	12.2	11.8	12.2
O	[% wt]	-	11.9	11.0	14.0
Lower heating value	[MJ/kg]	42.6	37.4	37.0	35.2
Density	[kg/m^3]	843.3	867.7	882.0	874.0
Molecular Weight	[g/mol]	226.0	270.1	292.2	229.1
Cetane number	[-]	52.0	62.0	51.3	59.3
Flash point	[°C]	66	163	159	113
Kinematic viscosity (40°C)	[mm^2/s]	2.5	4.6	4.3	2.8

Table 3 Gas analyser specification

Sensor/ Instrument	Range	Resolution	Uncertainty	Propagated Error
CO	0-4000 ppm	1 ppm	<100 ppm; ± 5 ppm >100 ppm; ± 5%	± 16.0%
NO	0-5000 ppm	1 ppm	<100 ppm; ± 5 ppm >100 ppm; ± 5%	± 7.5%
CO_2	0-20%	0.1 %	± 5.0% of reading	± 4.2%
O_2	0-30%	0.01%	± 0.2%	± 1.3%

Table 4 Operating conditions for all fuel types at $\phi = 0.65$

Fuel	$(A/F)_{stoich}$*	Fuel mass flow rate (g/s)	ALR	Atomising air mass flow rate (g/s)	Main air mass flow rate** (g/s)
Diesel	14.80	0.22	2.50	0.54	4.41
			2.25	0.49	4.46
			2.00	0.43	4.51
PME	12.38	0.24	2.50	0.61	4.03
			2.25	0.55	4.09
			2.00	0.49	4.15
SME	12.40	0.25	2.50	0.62	4.11
			2.25	0.56	4.17
			2.00	0.50	4.23
CME	12.08	0.27	2.50	0.67	4.31
			2.25	0.60	4.38
			2.00	0.54	4.45

* Stoichiometric air/fuel ratio by mass

** The flow rates shown are for establishment of flame at global equivalence ratio of $\phi = 0.65$.